IFN-Induced Protein with Tetratricopeptide Repeats 2 Inhibits Migration Activity and Increases Survival of Oral Squamous Cell Carcinoma

Kuo-Chu Lai,[1] Kuo-Wei Chang,[2] Chung-Ji Liu,[3] Shou-Yen Kao,[4] and Te-Chang Lee[1,2,5,6]

[1]Institute of Pharmacology and [2]Institute of Oral Biology, School of Dentistry, National Yang-Ming University; [3]Department of Oral and Maxillofacial Surgery, Mackay Memorial Hospital; [4]Department of Oral and Maxillofacial Surgery, Taipei Veterans General Hospital; [5]Institute of Biomedical Sciences, Academia Sinica; [6]National Research Institute of Chinese Medicine, Taipei, Taiwan, Republic of China

Abstract

The function of the IFN-stimulated gene family protein, IFN-induced protein with tetratricopeptide repeats 2 (IFIT2), is poorly understood. Here, we report that IFIT2 colocalizes with cytokeratin 18 in oral squamous cell carcinoma (OSCC) cells. Treatment of OSCC cells with IFN-β significantly increased the expression of IFIT2 and remarkably inhibited cell migration. To further explore the effect of IFIT2 on cell migration, IFIT2 expression was either silenced with a small interfering RNA or increased by ectopic expression. IFIT2 knockdown in OSCC cells led to a significantly higher level of migration *in vitro* ($P < 0.05$) compared with control cells; by contrast, IFIT2 overexpression led to a significantly lower level of migration *in vitro* ($P < 0.05$). Immunohistochemically, 71.4% of OSCC tissues had elevated IFIT2 protein levels compared with noncancerous matched tissues. Elevated IFIT2 protein expression was positively associated with tumor differentiation status and inversely associated with nodal stage in OSCC specimens ($P < 0.05$). Higher IFIT2 protein levels in tumor tissues were also associated with better patient survival ($P < 0.01$). Our present study shows an inverse correlation between IFIT2 expression and cell migration, suggesting that IFIT2 plays an important role in inhibiting this process and that its expression may be associated with better prognosis in patients with OSCC.
(Mol Cancer Res 2008;6(9):1431–9)

Introduction

Oral cancer is one of the major fatal diseases in the world, particularly in Europe, southern Africa, south-central Asia, Melanesia, and Australia (1). Oral cancer mortality ranks fifth among cancers in Taiwanese males and seventh in the world population since 1991 (2). More than 90% of cancers of the oral cavity are oral squamous cell carcinomas (OSCC). Patients with OSCC are generally treated by surgery, radiation therapy, or chemotherapy. However, the overall 5-year survival rate for OSCC patients has remained at 50% without significant improvement over the past 3 decades (3). Thus, a better understanding of the underlying molecular pathogenesis of oral cancer may yield more effective regimens for oral cancer treatment.

A causal association between betel quid chewing and oral cancer has been well documented (4). Using cultures of human keratinocytes (HaCaT cells), we previously reported that long-term exposure to sublethal doses of areca nut extracts (ANE; 0, 5, and 20 μg/mL for 35 passages) resulted in increased oxidative stress and genetic damage (5). We further adopted a colorimetric cDNA microarray technique (6) to compare gene expression profiles between long-term ANE-exposed HaCaT cells and untreated cells (Supplementary Fig. S1).[7] Among the many differentially expressed genes, IFN-induced protein with tetratricopeptide repeats 2 (*IFIT2*) drew our attention. The expression levels of IFIT2, which were confirmed by semiquantitative reverse transcription-PCR (RT-PCR), were significantly decreased in ANE-exposed cells compared with untreated cells (Supplementary Fig. S1).

IFIT2 is an IFN-stimulated gene (ISG) also known as *ISG54*, *GARG39*, and *MuP54* (7). IFNs are cytokines with pleiotropic properties, including antiviral, antitumor, and immunomodulatory activities (8). Notably, >300 ISGs have been identified in cells treated with IFNs (9). The products of ISGs mediate the diverse activities of IFNs, including regulation of transcription, proteasomal processing, apoptosis, antiviral and antiproliferative activities, and regulation of protein translation (9, 10). To date, only a few ISGs have been extensively studied. For example, ISG15, a critical antiviral molecule structurally and functionally similar to ubiquitin, is an endogenous tumor suppressor and may therefore serve as a therapeutic cancer target along with the molecules it regulates (11). ISG20, another antiviral protein with 3′ to 5′ exonuclease activity (12), also has therapeutic potential. As for IFIT2, it is not only one of the ISGs most responsive to IFNs but is also responsive to viruses and a variety of agents in cultured human and rodent cell lines (13, 14). Previous studies have shown

Received 3/17/08; revised 5/29/08; accepted 6/2/08.
Grant support: National Science Council, Taiwan, grants NSC 92-3112-B-010-024 and NSC 93-3112-B-001-036.
The costs of publication of this article were defrayed in part by the payment of page charges. This article must therefore be hereby marked *advertisement* in accordance with 18 U.S.C. Section 1734 solely to indicate this fact.
Note: Supplementary data for this article are available at Molecular Cancer Research Online (http://mcr.aacrjournals.org/).
Requests for reprints: Te-Chang Lee, Institute of Biomedical Sciences, No. 128, Section 2, Academia Road, Taipei 115, Taiwan, Republic of China. Phone: 886-2-26523055; Fax: 886-2-27829142. E-mail: bmtcl@ibms.sinica.edu.tw

doi:10.1158/1541-7786.MCR-08-0141

[7] Unpublished data.

that IFIT2 and IFIT1, the other known tetratricopeptide repeat-containing ISG, bind the translation initiation factor eIF3 and consequently inhibit initiation of protein synthesis (15). IFIT2 has also been reported to be an IFN-induced cytoskeleton-associated protein and plays an antiviral role in recombinant human IFN-γ treatment in human amnion-derived cells (16, 17). A recent study showed that IFIT2 colocalizes with β-tubulin *in vivo* and is enriched in the mitotic spindle of normal NIH3T3 cells and B16F10 melanoma cells undergoing mitosis (18). However, whether IFIT2 can regulate cell migration is unknown.

HaCaT cells are spontaneously immortalized but nontumorigenic human keratinocytes (19). IFIT2 gene expression is down-regulated on long-term exposure of HaCaT cells to ANE, implying that IFIT2 may inhibit the progression of malignancy. In the present study, we produced an antibody against IFIT2 to investigate its intracellular localization and possible functions in OSCC cells, particularly any possible inhibitory roles of IFIT2 on cell migration. In addition, we examined IFIT2 expression in OSCC tissues using immunohistochemistry and found an inverse association between tumor IFIT2 protein expression and 5-year survival of OSCC patients.

Results

Association of IFIT2 with Cytokeratin 18

To explore the biological function of IFIT2, we first examined the expression of the 54-kDa IFIT2 protein in various human cell lines by Western blotting. As shown in Fig. 1A, IFIT2 was significantly expressed in three OSCC cell lines, SAS, OC3, and SCC25, and in human keratinocyte HaCaT cells, but not in the OSCC cell line OECM-1 or in cell lines derived from human lung cancers, gastric cancer, or breast cancer. We examined the intracellular distribution of IFIT2 in HaCaT and SCC25 cells as well as normal human oral keratinocytes (passage 4) using immunohistostaining. IFIT2 staining was mainly localized in the cytoplasm in a fibrillar pattern similar to the pattern of cytoskeletal proteins (Fig. 1B). We further did optical serial sectioning with confocal microscopy of methanol-fixed SCC25 cells. We observed a cytoplasmic cytoskeletal staining pattern and a small amount of localized IFIT2 staining in the nucleus (Fig. 1C).

Actin filaments, microtubules, and intermediate filaments are the three major filament types of the cytoskeleton. We therefore examined the potential colocalization of IFIT2 with various cytoskeleton proteins using confocal microscopy. As shown in Fig. 2A, IFIT2 partially colocalized with cytokeratins and vimentin, but not with β-actin or α-tubulin, in SCC25 cells. Furthermore, a Western blot using a pan-cytokeratin antibody following immunoprecipitation of a SCC25 whole-cell lysate with anti-IFIT2 confirmed that low molecular weight cytokeratins coprecipitated with IFIT2 (Fig. 2B), indicating a physical interaction between IFIT2 and cytokeratins. Based on its molecular size, the lower cytokeratin band was suspected to be cytokeratin 18 (CK18). We confirmed a physical interaction between IFIT2 and CK18 by using a monoclonal antibody that recognizes both CK8 and CK18 to probe the proteins that were immunoprecipitated by the antibody against IFIT2 (Fig. 2C). When the immunoprecipitation/Western blot experiment was done in the reverse fashion, we also observed coprecipitation of

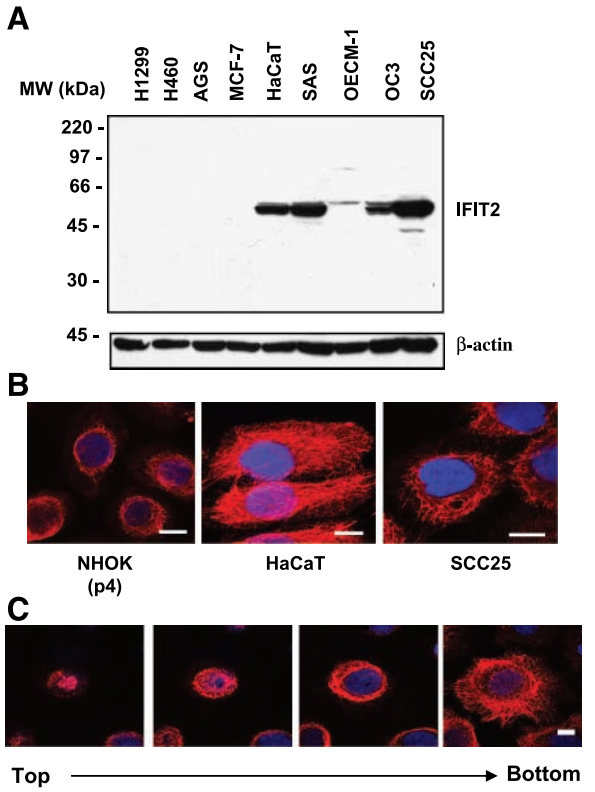

FIGURE 1. Endogenous expression and subcellular localization of IFIT2. **A.** Western blot analysis of IFIT2 levels in various human cell lines. Total cellular protein (25 μg) isolated from human lung cancer cell lines (H1299 and H460), gastric cancer cell line (AGS), breast cancer cell line (MCF-7), human keratinocyte cell line (HaCaT), and OSCC cell lines (SAS, OECM-1, OC3, and SCC25) was loaded in each lane of the SDS-polyacrylamide gel for electrophoresis and subsequently immunoblotted with anti-IFIT2. β-Actin was analyzed as a loading control. **B.** Immunofluorescence staining of IFIT2 in normal human oral keratinocytes, passage 4 (*NHOK*, *p4*), HaCaT, and SCC25 cells. Scale bar, 10 μm. **C.** Optical serial sections of IFIT2 immunostaining (*red*) and 4′,6-diamidino-2-phenylindole counterstaining (*blue*) of an SCC25 cell were collected by confocal microscopy. The depth of the images from the top of the cell was 1.5, 3.0, 4.5, and 6.0 μm, from left to right. Scale bar, 10 μm.

IFIT2 with CK8 and CK18 by the anti-CK8 and CK18 monoclonal antibody (Fig. 2D). Based on molecular sizes, these results show that IFIT2 interacts with cytokeratins, and likely with CK18.

Migration Inhibition by Elevated Expression of IFIT2

Because cytoskeletal proteins play a crucial role in regulating cellular migration, we asked whether migration of OSCC cells was reduced by increased expression of IFIT2. Because OC3 cells express relatively low levels of IFIT2 compared with SCC25 cells, we first treated OC3 cells with various concentrations of IFN-β for 24 or 48 h. IFN-β treatment at the dose range of 100 to 500 units/mL for 24 h induced an obvious increase in the amount of IFIT2 mRNA and protein in OC3 cells without causing marked toxicity (Fig. 3A and B). However, IFN-β markedly inhibited OC3 cell growth if the treatment time was lengthened to 48 h. These results indicate that IFIT2 expression could be enhanced by treatment with IFN-β at the dose range used without significant growth

inhibition (Fig. 3B). To examine the effect of IFN-β on OC3 cell migration, we treated OC3 cells with or without IFN-β at a dose of 500 units/mL for 24 h and then seeded equal numbers of cells onto modified Boyden chambers. Treatment of OC3 cells with IFN-β significantly decreased the migration of OC3 cells by 2.0-fold ($P < 0.01$) compared with untreated cells (Fig. 3C). As expected, the total number of untreated cells and cells treated with IFN-β was not different at the end of the 15-h incubation in the Boyden chambers (data not shown). Similar results were obtained in OECM-1 cells (Supplementary Fig. S2). SCC25 cells, which contain a high abundant amount of IFIT2, were not responsible to treatment with IFN-β at either IFIT2 expression or reduction of cell migration (Supplementary Fig. S2). To confirm whether IFIT2 is involved in IFN-β–induced migration inhibition, we did similar experiments in OC3 cells transfected with control or IFIT2 small interfering RNA (siRNA). As shown in Fig. 3D, transfection of IFIT2 siRNA abolished the effects of IFN-β on IFIT2 induction as well as migration inhibition. However, transfection of control siRNA into OC3 cells did not interfere with the activities of IFN-β on IFIT2 induction and migration inhibition ($P < 0.05$; Fig. 3D).

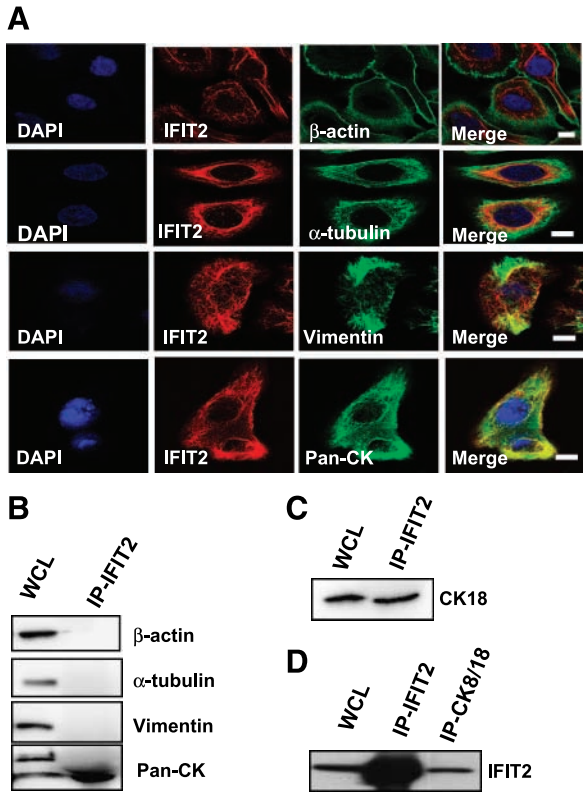

FIGURE 2. Interaction of IFIT2 with CK18 in SCC25 cells. SCC25 cells were grown on coverslips and stained with various primary antibodies and Alexa Fluor 488–conjugated or rhodamine-conjugated secondary antibodies for immunofluorescence as described in Materials and Methods. **A.** Cultured SCC25 cells grown on coverslips were costained with anti-IFIT2 and anti-β-actin, anti-α-tubulin, anti-vimentin, or anti-pan-cytokeratin (*Pan-CK*) and counterstained with 4′,6-diamidino-2-phenylindole (*DAPI*). Scale bars, 10 μm. **B.** Coimmunoprecipitation and Western blot analysis of IFIT2-interacting proteins. SCC25 whole-cell lysates (*WCL*) were immunoprecipitated with anti-IFIT2 (*IP-IFIT2*) and immunoblotted with antibodies against β-actin, α-tubulin, vimentin, or pan-cytokeratin. **C.** Coimmunoprecipitation and Western blot analysis of IFIT2 and CK8 and CK18. A similar experiment as described in **B** was done, except that the immunoprecipitates were immunoblotted with antibody against CK8. **D.** SCC25 whole-cell lysates were immunoprecipitated with anti-CK8 and CK18 (*IP-CK8/18*) and immunoblotted with anti-IFIT2. All experiments were done thrice, and one representative experiment is shown.

To further corroborate the involvement of IFIT2 in modulating cell migration, we did migration experiments using OSCC cells in which IFIT2 expression was either decreased by small RNA interference technique or increased by ectopic expression. As shown in Fig. 4A, IFIT2 mRNA was markedly reduced in SCC25 cells transfected with IFIT2 siRNA for 24, 48, and 72 h compared with control siRNA cells transfected with a siRNA that targeted the luciferase gene. IFIT2 protein levels in SCC25 cells transfected with IFIT2 siRNA were reduced to approximately 40% and 50% at 72 and 96 h after transfection, respectively, compared with those of SCC25 cells transfected with control siRNA (Fig. 4B), indicating that the IFIT2 protein has a longer turnover time than its mRNA. As shown in Fig. 4C, IFIT2 siRNA transfection significantly increased migration by 2.0-fold compared with SCC25 cells transfected with control siRNA ($P < 0.05$). In contrast, ectopic expression of FLAG-tagged IFIT2 in HEK293T cells by transfection with pFLAG-CMV22-IFIT2 resulted in increased expression of IFIT2 and a ~32% decrease in migration ($P < 0.05$; Fig. 5A). Similarly, OECM-1 cells transfected with pcDNA-HA2-IFIT2 showed increased expression of IFIT2 but a ~36% decrease in migration by the Transwell migration assay compared with OECM-1 cells transfected with the control pcDNA-HA2 plasmid ($P < 0.05$; Fig. 5B). Furthermore, OECM-1 cells overexpressing HA-tagged IFIT2 exhibited significantly less migration potential by a wound-healing assay than control cells ($P < 0.05$; Supplementary Fig. S3). These results show that IFIT2 modulates migration of OSCC cells.

Higher Expression of IFIT2 in OSCC Tissues Correlates with Better Patient Survival

We also compared IFIT2 mRNA levels in 20 OSCC tumor and noncancerous matched tissue (NCMT) pairs using semiquantitative RT-PCR. We found that 95% of the OSCC tissues expressed higher levels of IFIT2 mRNA than their NCMT counterparts (Supplementary Fig. S4). To confirm the enhanced expression of IFIT2 in OSCC tissues, we did immunohistochemical staining with anti-IFIT2 on another 35 pairs of OSCC tissues and their NCMTs. As shown in the representative images in Fig. 6A (*a*), IFIT2 expression in the control NCMTs was faint and mainly observed in superficial cells. However, strong immunoreactivity against IFIT2 was observed in tumor cells in most OSCC tissues (Fig. 6A, *b-d*) but not in inflammatory cells. Among these 35 tissue pairs, most of the OSCC tissues (71.4%) exhibited stronger immunoreactivity to IFIT2 than did their corresponding NCMTs, a few (5.7%) of the OSCC tissue samples showed weaker IFIT2 immunoreactivity than their NCMTs, and the remaining 22.9% of OSCC and NCMT pairs had similar IFIT2 levels.

To investigate the association of clinicopathologic features with IFIT2 expression in OSCC tissues, we assessed IFIT2 levels immunohistochemically in tumors from 53 OSCC patients who had received curative surgery between 2000 and

2006 and were followed up for 2 to 75 months. IFIT2 expression levels in 53 OSCC tissues were classified into low (negative to moderately positive immunostaining) and high (strongly positive immunostaining) IFIT2 expression groups. Among these 53 patients, 73.6% (39 cases) had OSCC tissue with high IFIT2 expression and 26.4% (14 cases) had OSCC tissue with low IFIT2 expression. The associations between IFIT2 expression (as determined via immunohistochemistry) and several clinicopathologic features for these 53 patients are summarized in Table 1. A higher percentage of patients with tumors expressing elevated levels of IFIT2 were classified with a lymph node stage of N0 than with N1-3 stage classification (N0 versus N1-3; $P < 0.05$). Likewise, a higher percentage of patients expressing elevated levels of IFIT2 were classified as having good differentiated tumors than having moderately or poorly differentiated tumors (moderate and poorly versus good; $P < 0.05$). However, there was no significant association between IFIT2 expression level and tumor stage or clinical stage. The influence of IFIT2 expression on survival time in 48 of 53 patients (5 patients have no survival time data) was determined using Kaplan-Meier plots. Patients with high IFIT2 expression had significantly better postsurgery survival (median, 66.5 months) than those with low IFIT2 expression (median, 18.9 months; $P < 0.01$; Fig. 6B). Because most of the OSCC patients recruited in this study were diagnosed at stage IV, we did similar analysis with stage IV OSCC patients. The median postsurgery life span for stage IV patients with high IFIT2 expression remained to be 66.5 months, whereas that for low IFIT2 expression was 13.6 months ($P < 0.01$; Fig. 6C). These results indicate that OSCC patients expressing high levels of IFIT2 have a better prognosis than those expressing low levels of IFIT2.

Discussion

In the present study, we modulated IFIT2 protein levels by siRNA and ectopic expression and showed that IFIT2 is a negative regulator of migratory activity of OSCC cells. Using immunohistochemical staining and immunoprecipitation, the intracellular IFIT2 protein mainly colocalized with

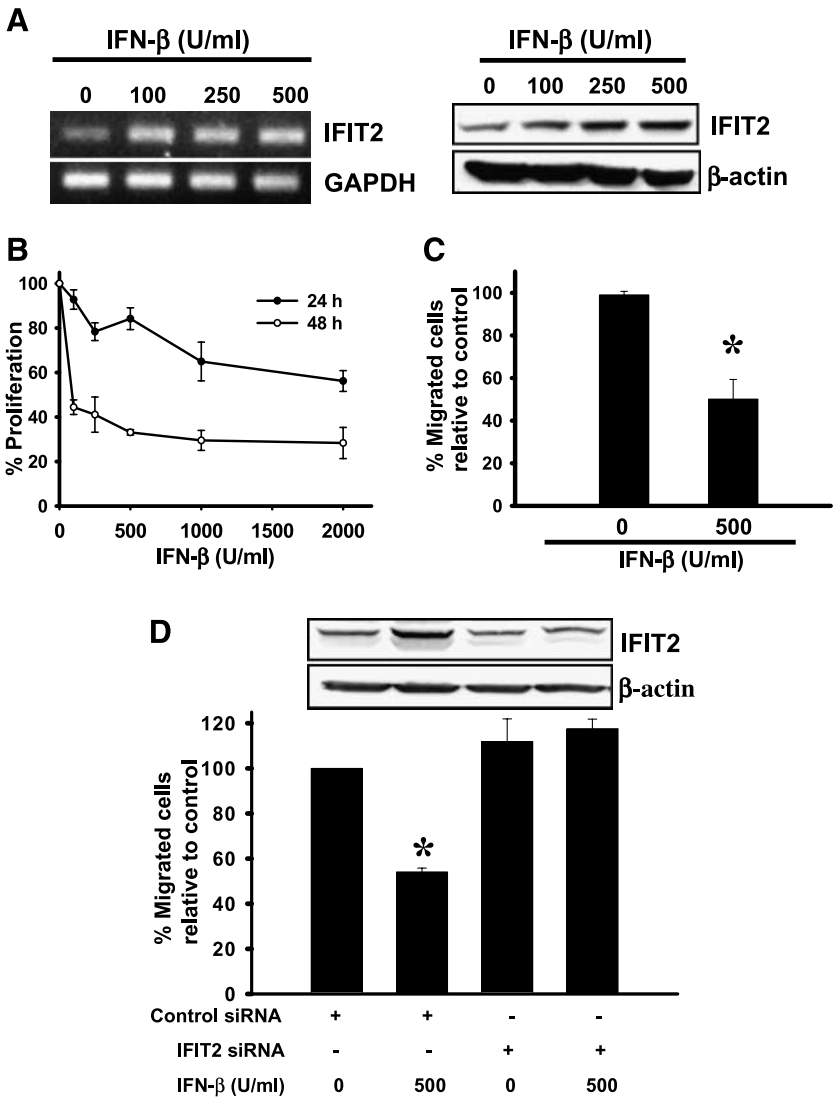

FIGURE 3. IFN-β reduces cell migration through IFIT2 expression. **A.** Enhanced expression of IFIT2 following IFN-β treatment. Logarithmically growing OC3 cells were treated with various concentrations of IFN-β for 24 h. RT-PCR (*left*) and Western blot (*right*) analysis of IFIT2 in OC3 cells treated with various doses of IFN-β (0-500 units/mL). At the end of treatment, the amount of IFIT2 induced by IFN-β was analyzed by RT-PCR (*GAPDH* was used as the loading control) and Western blotting (β-actin was used as the loading control). All experiments were done thrice, and one representative experiment is shown. **B.** Antiproliferation effect of IFN-β on OC3 cells. Cells were treated with various concentrations of IFN-β for 24 or 48 h. Cells were counted and examined for viability by trypan blue dye exclusion. Points, average of three independent experiments; bars, SD. **C.** Migration inhibition of IFN-β on OC3 cells. Cells were seeded in the upper chamber of a Transwell cell culture system, and after 15 h, the number of IFN-β–treated cells that had migrated across the membrane was counted and normalized with respect to the migration of untreated cells. All experiments were done thrice and in triplicate. Bars, SD. *, $P < 0.05$, by Student's *t* test (two sided). **D.** Logarithmically growing OC3 cells were transfected with control or IFIT2 siRNA followed by IFN-β treatment at 500 units/mL for 24 h. At the end of treatment, the amount of IFIT2 induced by IFN-β was analyzed by Western blotting assay (β-actin was used as the loading control). All experiments were done thrice, and one representative experiment is shown. Cells were then seeded in the upper chamber of a Transwell cell culture system, and after 15 h, the number of IFN-β–treated cells that had migrated across the membrane was counted and normalized with respect to the migration of untreated cells. All experiments were done thrice and in triplicate. Bars, SD. *, $P < 0.05$, by Student's *t* test (two sided).

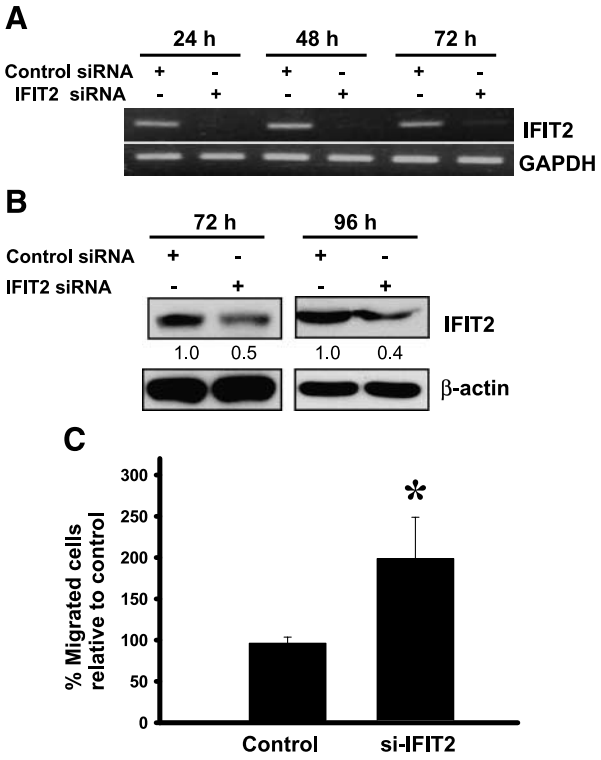

FIGURE 4. Effect of reduced IFIT2 expression by siRNA-mediated knockdown on *in vitro* migration of SCC25 cells. **A.** RT-PCR analysis of IFIT2 in SCC25 cells transfected with 200 pmol IFIT2 siRNA or control luciferase gene siRNA for 24, 48, and 72 h. *GAPDH* was used as the loading control. **B.** Western blot analysis of IFIT2 expression in SCC25 cells transfected with IFIT2 siRNA or control siRNA for 72 and 96 h. β-Actin was used as the loading control. All experiments were done thrice, and one representative experiment is shown. **C.** Migration analysis of SCC25 cells treated with IFIT2 siRNA. After a 72-h transfection with IFIT2 siRNA, SCC25 cells were then seeded in the upper chamber of a Transwell cell culture system, and after 15 h, the number of IFIT2 siRNA-transfected cells (*si-IFIT2*) that had migrated across the membrane was counted and normalized with respect to the migration of control siRNA-transfected cells. All experiments were done thrice and in triplicate. Bars, SD. *, $P < 0.05$, by Student's *t* test (two sided).

cytokeratins, forming a fibrillar structure in the cytosol. Our results show that in OSCC cells, IFIT2, which contains a tetratricopeptide repeat, a structural domain widely involved in protein-protein interactions (20), likely interacts with CK18, which is usually paired with CK8 and normally expressed in all simple epithelia but not in stratified epithelia (21). Recent evidence suggests that CK18 may serve as one of the biological markers for micrometastasis of gastric carcinoma (22, 23). In addition, aberrant expression of CK8 and CK18 is frequently observed in squamous cell carcinoma derived from stratified epithelia (21, 24) and in adenocarcinomas and basal cell carcinomas (25). Although the contribution of anomalous expression of CK8 and CK18 to a malignant cancer phenotype is not clear, our results of an interaction between IFIT2 and CK18 suggest that IFIT2 may mediate through CK18 resulting in an alteration in the phenotypic characteristics of squamous cell carcinoma, such as a reduced migratory activity.

A variety of CK18-binding proteins have been identified, including tumor necrosis factor receptor 2, tumor necrosis factor receptor 1–associated death domain protein, death effector domain-containing protein, and Mrj, a member of the DnaJ/heat shock protein 40 family (26). Mrj works together with Hsp/c70 as a CK18-specific cochaperone and plays a crucial role in the regulation of CK8/18 filament organization (27). Therefore, whether IFIT2 acts as an adaptor protein between heat shock proteins and CK18 to modulate the activity of CK18 needs to be addressed. Although the detailed mechanism of IFIT2-cytokeratin interactions is unknown, tetratricopeptide repeat–containing proteins have been shown to associate with heat shock protein 70 and heat shock protein 90 and act as cochaperones to regulate protein structure, stability, and degradation (28).

The major clinical oncologic problem for cancer patients is metastasis of tumor cells from the primary tumor to secondary sites. Metastasis is a sequential process by which tumor cells disseminate from the primary tumor, migrate through the basement membrane, survive transport through the circulatory system, invade a secondary site, and start to proliferate (29). Importantly, the frequency of metastasis strongly correlates with the migration potential of primary tumor cells (30). In the present study, we found that IFIT2 negatively controlled the migration of OSCC cells, and hence, higher IFIT2 expression was positively associated with low lymph node stage and 5-year survival rate.

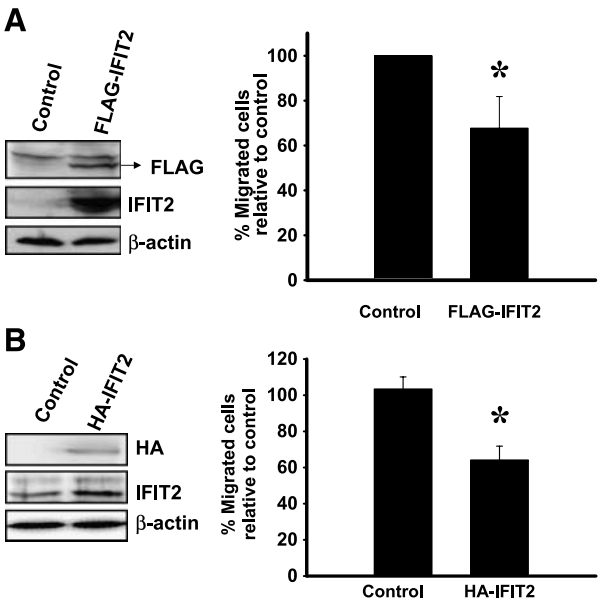

FIGURE 5. Reduced migration of cells on ectopic expression of IFIT2. **A.** HEK293T cells were transfected with pFLAG-CMV22-IFIT2 (*FLAG-IFIT2*) or pFLAG-CMV22 plasmid (*Control*) for 72 h. Left, Western blot analysis of IFIT2 and FLAG-tagged IFIT2 expression in vector control cells and FLAG-IFIT2–expressing cells; right, a migration assay was done to compare cell migration between control and pFLAG-CMV22-IFIT2–expressing cells. **B.** OECM-1 cells were transfected with pcDNA-HA2-IFIT2 (*HA-IFIT2*) or pcDNA-HA2 plasmid (*Control*) for 72 h. Left, Western blot analysis of IFIT2 and HA-tagged IFIT2 expression in vector control cells and HA-IFIT2–expressing cells; right, a migration assay was done to compare cell migration between control and HA-IFIT2–expressing cells. For Western blot analysis, β-actin was analyzed as the loading control. All experiments were done thrice and in triplicate. Bars, SD. *, $P < 0.05$, by Student's *t* test.

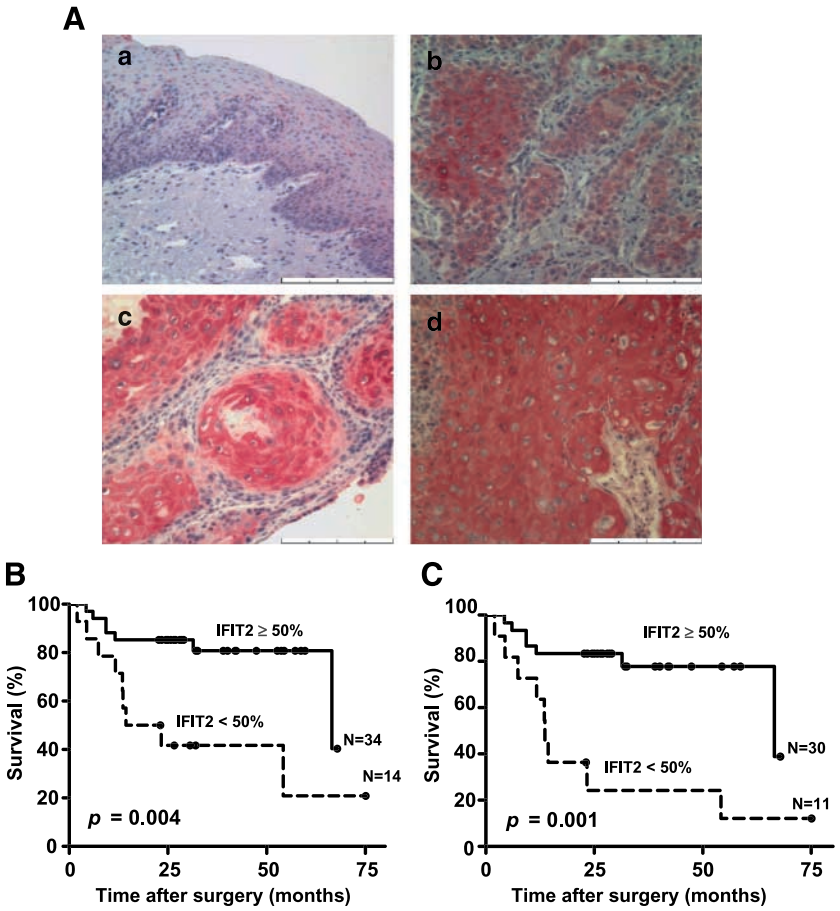

FIGURE 6. Enhanced expression of IFIT2 in OSCC tissues. **A.** Representative immunohistochemical staining of IFIT2 in patient tissues. Scale bars, 200 μm. a, a NCMT exhibited weak immunostaining, mainly in superficial cells; b to d, OSCC tissues exhibited strong immunostaining. The tissues shown in a and b were obtained from the same patient. **B.** Association of IFIT2 expression levels with survival time in OSCC patients. The survival time of 48 patients was analyzed by Kaplan-Meier plots. The patients were divided into two groups based on IFIT2 immunostaining: a high-IFIT2 expression group, having positive IFIT2 immunostaining in ≥50% of the cells analyzed, and a low-IFIT2 expression group, having positive IFIT2 immunostaining in <50% of the cells analyzed. **C.** The survival time of 41 patients with stage IV was analyzed by Kaplan-Meier plots. The patients were divided into two groups as described in **B**.

The cause of the overexpression of IFIT2 in OSCC tissues and whether IFIT2 is involved in development of OSCC are unclear at present. However, it is well established that IFIT2 is activated through an IFN-stimulated response element–dependent mechanism by type I IFN (31) and other agents, including poly(deoxyinosinic-deoxycytidylic acid), interleukin-1 (32), viral infection (13), retinoic acid (33), and lipopolysaccharide (34). Several studies have pointed out that human papillomavirus infection is associated with increased risk of oral cancer, independent of exposure to tobacco and alcohol (35, 36). Therefore, up-regulations of ISGs, including IFIT2, at the tumor site could be caused by IFNs produced in response to ongoing viral replication in adjacent tissue, as reported for nasopharyngeal carcinoma patients with EBV infection (37). Whether the enhanced expression of IFIT2 in OSCC tissues is due to the inflammatory response to viral infection or chemicals warrants further investigations. Our current findings showed that patients with OSCC have a better prognosis if IFIT2 is overexpressed in OSCC tissues. Therefore, we suspect that IFIT2 may impart certain growth advantages for cancer development but not for malignant progression. In our preliminary studies shown in Supplementary Fig. S1, IFIT2 was remarkably reduced by long-term exposure of HaCaT cells to ANE, implying that chronic exposure to ANE, a carcinogen for oral cancer, may suppress the expression of IFIT2, leading to increased migration activity and possibly malignancy.

IFNs have been evaluated as therapeutic agents against several malignancies, including melanoma and chronic myelogenous leukemia (38, 39). In this study, we showed that IFIT2 expression was increased and cell migratory ability was inhibited at 500 units/mL of IFN-β in OC3 and OECM-1 cells that expressed relatively low levels of IFIT2. Whether IFN-β is a potential agent against OSCC invasiveness warrants further investigation.

In conclusion, increased expression of IFIT2 could inhibit the migration of OSCC cells, and the positive association of IFIT2 expression levels and increased life span of OSCC patients is probably associated with reduced migration of tumor cells. Meanwhile, increased IFIT2 expression is also significantly associated with low lymph node stage and good tumor differentiation in patients with OSCC. As expected, higher IFIT2 protein levels in tumor tissues are associated with better patient survival. These findings significantly expand our understanding of IFIT2 function by suggesting that IFIT2 plays an important role in the modulation of cell migration, which may be responsible for better prognosis in OSCC patients.

Materials and Methods

Antibodies

A polyclonal antibody against IFIT2 was prepared by IgMedica Biotechnology Co. using a synthetic peptide

containing residues 403 to 426 of human IFIT2. This antibody specifically recognized a protein with a molecular weight of 54 kDa in cells ectopically expressing IFIT2. Monoclonal anti-pan-cytokeratin (for detection of CK4, CK5, CK6, CK10, CK13, and CK18) and anti-CK8 and CK18, which recognizes both CK8 and CK18, were obtained from Santa Cruz Biotechnology, anti-β-actin was purchased from Abcam, anti-α-tubulin was purchased from Calbiochem, anti-vimentin was obtained from BD PharMingen, anti-HA.11 was from Covance, anti-FLAG was from Sigma, and horseradish peroxidase–conjugated anti-mouse and anti-rabbit IgG secondary antibodies were obtained from Chemicon International.

Cell Culture, Treatment, and Cell Viability

Human embryonic kidney 293T cell line HEK293T (American Type Culture Collection) was grown at 37°C in DMEM (Invitrogen Life Technologies) supplemented with 10% fetal bovine serum and antibiotics. OECM-1 cells, a human oral epidermoid carcinoma cell line (obtained from Dr. C-L. Meng, National Defense Medical College, Taipei, Taiwan), were grown in RPMI 1640 containing 10% fetal bovine serum and antibiotics (Invitrogen Life Technologies). OC3 cells, a human oral carcinoma cell line, were established and cultured as described (40). SCC25 cells (American Type Culture Collection) were cultured at 37°C in a 1:1 mix of DMEM and Ham F12 medium (Invitrogen Life Technologies) containing 10% fetal bovine serum, 400 ng/mL hydrocortisone, and antibiotics. To determine the antiproliferative effect of IFN-β on oral cancer cells, 1×10^5 OC3 cells were plated onto six-well plates and incubated overnight. The cells were treated with various concentrations of IFN-β1a (PBL Biomedical Laboratories) for 24 or 48 h. Cell viability was determined by the trypan blue dye exclusion method.

Immunofluorescence Staining and Confocal Microscopy

Cells grown on glass coverslips were fixed with ice-cold methanol for 20 min at −20°C, washed with PBS [7.9 mmol/L Na_2HPO_4, 1.5 mmol/L KH_2PO_4, 2.7 mmol/L KCl, and 137 mmol/L NaCl (pH 7.4)], and incubated with antibodies against IFIT2 (1:100 dilution), β-actin (1:100 dilution), α-tubulin (1:50 dilution), vimentin (1:30 dilution), or pan-cytokeratins (1:100 dilution) in 1× TBBS buffer [20 mmol/L Tris, 500 mmol/L NaCl (pH 7.5), 0.1% (v/v) Tween 20] containing 3% (w/v) bovine serum albumin for 1 h at 37°C. The coverslips were then washed thrice with PBS and further incubated with either rhodamine-coupled (for IFIT2 visualization) or Alexa Fluor 488–coupled (for β-actin, α-tubulin, vimentin, and pan-cytokeratin) secondary antibodies (Molecular Probes, Invitrogen). After counterstaining with 4′,6-diamidino-2-phenylindole (Sigma-Aldrich), the coverslips were subjected to confocal image analysis (Radiance 2100 System, Bio-Rad). Optical serial sectioning was done from top to bottom.

Western Blot Analysis

Equal amounts of cell extracts were electrophoretically separated on 10% SDS-PAGE gradients gels, transferred onto polyvinylidene difluoride membranes (Amersham Biosciences, GE Healthcare Bio-Sciences Corp.), and incubated at 4°C overnight with primary antibodies at an appropriate dilution. The membranes were then incubated with horseradish peroxidase–conjugated anti-rabbit or anti-mouse secondary antibody for 1 h at room temperature. Membrane-bound antibody was then visualized by chemiluminescence using SuperSignal West Pico chemiluminescence reagent (Pierce) on Kodak BioMax MR film (Eastman Kodak). The dilution of primary antibodies was as follows: anti-IFIT2, 1:5,000; anti-CK8 and CK18, 1:500; anti-HA, 1:1,000; anti-FLAG, 1:1,000; and anti-β-actin, 1:5,000. Western blot band intensity was analyzed with MetaMorph Offline software (Universal Imaging).

Immunoprecipitation

Logarithmically growing cells were washed twice with ice-cold PBS and resuspended in 1 mL radioimmunoprecipitation assay lysis buffer [50 mmol/L Tris-HCl (pH 8.0), 150 mmol/L NaCl, 1 mmol/L sodium orthovanadate, 1% (w/v) NP40, 0.5% (w/v) sodium deoxycholate, 0.1% (w/v) SDS] supplemented with 20 μL protease inhibitor cocktail (Roche Diagnostics GmbH). Total protein concentration was determined by Bradford assay using the Bio-Rad protein assay reagent with bovine serum albumin as the standard. An aliquot of cell extract was incubated with anti-IFIT2 immobilized on protein A-Sepharose CL-4B beads (Amersham Pharmacia Biotech)

Table 1. Association of IFIT2 Expression Levels with Clinicopathologic Features in 53 Patients with OSCC

Variable	No. Cases	IFIT2 <50%,* *n* (%)	IFIT2 ≥50%,* *n* (%)	*P* †
Tumor stage				
T1-3	13	5 (38.5)	8 (61.5)	0.292
T4	40	9 (22.5)	31 (77.5)	
Lymph node stage				
N0	25	3 (12.0)	22 (88.0)	0.032
N1-3	28	11 (39.2)	17 (60.8)	
Clinical stage				
I-III	9	3 (33.3)	6 (66.7)	0.684
IV	44	11 (25.0)	33 (80.0)	
Tumor differentiation status				
Moderate + poor	29	11 (37.9)	18 (62.1)	0.023
Good	22	2 (9.1)	20 (90.0)	

*The patients were divided into two groups based on IFIT2 immunostaining: a high-IFIT2 expression group, having positive IFIT2 immunostaining in ≥50% of the cells analyzed, and a low-IFIT2 expression group, having positive IFIT2 immunostaining in <50% of the cells analyzed.
†Fisher's exact test (two sided).

overnight at 4°C with gentle rotation. Beads were extensively washed four times with wash buffer [50 mmol/L Tris-HCl (pH 7.4), 300 mmol/L NaCl, 5 mmol/L EDTA, 1% (w/v) Triton X-100], boiled in SDS sample buffer (125 mmol/L Tris-HCl, 4% SDS, 20% glycerol, 10% 2-mercaptoethanol, 0.004% bromphenol blue), and centrifuged at 12,000 × *g* for 5 min. Supernatants were immediately subjected to Western blot analysis as described above.

Semiquantitative RT-PCR

Total RNA was extracted from cultured cells using Tri-reagent (Sigma) followed by treatment with DNase I (Invitrogen Life Technologies) to remove contaminating DNA. An aliquot of 2.5 μg total RNA was subjected to semiquantitative RT-PCR using Taq DNA Polymerase (TaKaRa) with amplification conditions as follows: incubation at 94°C for 5 min followed by 35 cycles of 94°C for 30 s, 54°C for 30 s, and 72°C for 30 s, with a final incubation at 72°C for 10 min. The PCR products were examined by electrophoresis on a 2% agarose gel and stained with ethidium bromide. The respective forward and reverse primers used for amplification were 5′-ACAAGGCCATCCACCACTTTAT-3′ and 5′-CCCAGCAATTCAGGTGTTAACA-3′ for *IFIT2* and 5′-TGGTATCGTGGAAGGACTCA-3′ and 5′-AGTGGGTGTCGCTGTTGAAG-3′ for the glyceraldehyde-3-phosphate dehydrogenase gene (*GAPDH*, loading control).

RNA Interference

siRNA duplexes were synthesized by Proligo Singapore Pte. Ltd. SCC25 cells were plated at a density of 2×10^5 per 60-mm dish 1 d before transfection. siRNA was transfected into the cells using Lipofectamine 2000 reagent (Invitrogen) according to the instructions of the manufacturer. The siRNA sequence for targeting IFIT2 mRNA was 5′-CCAAAGAACCCAGAAUUCATT-3′ (si-IFIT2). A double-stranded RNA (5′-CGUACGCGGAAUACUUCGATT-3′) targeting the luciferase gene was used as a negative control. Migration activity and Western blot assays were done at either 72 or 96 h after transfection of siRNA into the cells.

Plasmids and Transfection

To construct tagged IFIT2 expression vectors, we subcloned the full-length IFIT2 cDNA into the *Not*I and *Bam*HI sites of pFLAG-CMV22 (Sigma) and pcDNA-HA2 plasmid (kindly provided by Dr. J-Y. Chen, Institute of Biomedical Sciences, Academia Sinica, Taipei, Taiwan). The respective forward and reverse primers for the pFLAG-CMV22 plasmid and pcDNA-HA2 plasmid were 5′-TTGCGGCCGCAATGAGTGAGAACAATAAGA-3′ and 5′-CGCGGATCCGCAGTAGCCTAGTGGGCACCA-3′, and 5′-CGCGGATCCGCGATGAGTGAGAACAATAAG-3′ and 5′-AACGCCGGCGTTTCAGCAGTAGCCTAGTGG-3′ for the full-length *IFIT2* gene. The pFLAG-CMV22-IFIT2 plasmid, the pcDNA-HA2-IFIT2 plasmid, or their empty vectors were separately transfected into HEK293T and OECM-1 cells, respectively, using FuGENE HD transfection reagent (Roche Diagnostics) according to the instructions of the manufacturer. For transfection experiments, pEGFPN-1 (BD Biosciences Clontech) plasmid was adopted to monitor the transfection efficiency. Under our experimental conditions, the transfection efficiencies were >70% by examining the GFP-positive cells under a fluorescence microscope. Migration activity and Western blot assays were done at 72 h after transfection.

Transwell Migration Assay

The Boyden chamber system was used to evaluate the effects of IFIT2 expression and IFN-β on migration. In brief, 2×10^4 cells suspended in 100 μL medium without fetal bovine serum were seeded in the upper chamber of a Transwell plate containing a membrane with 8-μm pores (Corning Costar) precoated with 1% gelatin (Merck), and the lower chamber was filled with medium containing 10% fetal bovine serum. After 15 h of incubation, cells on the top side of the upper Transwell membrane were removed with Q-tips. The cells trapped on the bottom side of the membrane were fixed and stained with 4′,6-diamidino-2-phenylindole (5 ng/mL) for 10 min. The number of cells from eight different areas of each membrane was counted under a fluorescence microscope and averaged. Three membranes were tested for IFN-β dose or each transfectant.

Tissue Samples and Immunohistochemical Staining

Tissue samples previously collected at the Mackay Memorial Hospital (Taipei, Taiwan) were used with the approval of the Mackay Memorial Hospital's Institutional Review Board. In this study, tissue arrays containing 53 primary OSCC tissues and 35 paired NCMTs were used for immunohistochemistry. In brief, 5-μm-thick tissue sections were dewaxed, rehydrated, and then incubated with polyclonal anti-IFIT2 (1:400 dilution) in a humidification chamber at 4°C overnight. After rinsing with PBS, standard immunohistochemical staining was done using an LSAB2 streptavidin-biotin complex system (Dako Corp.) with aminoethylcarbazole as the chromogen and subsequently counterstained with hematoxylin and mounted with Clearmount (Zymed Laboratories, Inc.). The immunoreactivity of IFIT2 was determined based on the average percentage of positively stained cells in 10 randomly selected high-power fields. The specimens were arbitrarily defined as negative if immunoreactivity was observed in <10% of the cells, as moderately positive if immunoreactivity was observed in between 10% and 50% of the cells, and as strongly positive if the immunoreactivity was present in ≥50% of the cells.

Statistical Methods

Fisher's exact test was used to examine the statistical significance of associations between IFIT2 expression levels and clinicopathologic features. The Kaplan-Meier method was used to estimate overall patient survival, and the log-rank test was used to compare overall survival among different patient groups. Student's *t* test was used to determine the statistical significance of the differences between experimental groups; *P* values of <0.05 were considered statistically significant, and all *P* values were two sided.

Disclosure of Potential Conflicts of Interest

No potential conflicts of interest were disclosed.

Acknowledgments

We thank Drs. Ling-Huei Yih and Jeng-Fan Lo for critical review of the manuscript.

References

1. Parkin DM, Bray F, Ferlay J, Pisani P. Global cancer statistics, 2002. CA Cancer J Clin 2005;55:74–108.

2. Hsieh LL, Wang PF, Chen IH, et al. Characteristics of mutations in the p53 gene in oral squamous cell carcinoma associated with betel quid chewing and cigarette smoking in Taiwanese. Carcinogenesis 2001;22:1497–503.

3. Cooper JS, Pajak TF, Forastiere AA, et al. Postoperative concurrent radiotherapy and chemotherapy for high-risk squamous-cell carcinoma of the head and neck. N Engl J Med 2004;350:1937–44.

4. Jeng JH, Chang MC, Hahn LJ. Role of areca nut in betel quid-associated chemical carcinogenesis: current awareness and future perspectives. Oral Oncol 2001;37:477–92.

5. Lai KC, Lee TC. Genetic damage in cultured human keratinocytes stressed by long-term exposure to areca nut extracts. Mutat Res 2006;599:66–75.

6. Chen JJ, Wu R, Yang PC, et al. Profiling expression patterns and isolating differentially expressed genes by cDNA microarray system with colorimetry detection. Genomics 1998;51:313–24.

7. Levy D, Larner A, Chaudhuri A, Babiss LE, Darnell JE, Jr. Interferon-stimulated transcription: isolation of an inducible gene and identification of its regulatory region. Proc Natl Acad Sci U S A 1986;83:8929–33.

8. Goodbourn S, Didcock L, Randall RE. Interferons: cell signalling, immune modulation, antiviral response and virus countermeasures. J Gen Virol 2000;81:2341–64.

9. de Veer MJ, Holko M, Frevel M, et al. Functional classification of interferon-stimulated genes identified using microarrays. J Leukoc Biol 2001;69:912–20.

10. Williams BR. Transcriptional regulation of interferon-stimulated genes. Eur J Biochem 1991;200:1–11.

11. Andersen JB, Hassel BA. The interferon regulated ubiquitin-like protein, ISG15, in tumorigenesis: friend or foe? Cytokine Growth Factor Rev 2006;17:411–21.

12. Nguyen LH, Espert L, Mechti N, Wilson DM III. The human interferon- and estrogen-regulated ISG20/HEM45 gene product degrades single-stranded RNA and DNA *in vitro*. Biochemistry 2001;40:7174–9.

13. Zhu H, Cong JP, Shenk T. Use of differential display analysis to assess the effect of human cytomegalovirus infection on the accumulation of cellular RNAs: induction of interferon-responsive RNAs. Proc Natl Acad Sci U S A 1997;94:13985–90.

14. Bluyssen HA, Vlietstra RJ, van der Made A, Trapman J. The interferon-stimulated gene 54 K promoter contains two adjacent functional interferon-stimulated response elements of different strength, which act synergistically for maximal interferon-α inducibility. Eur J Biochem 1994;220:395–402.

15. Terenzi F, Hui DJ, Merrick WC, Sen GC. Distinct induction patterns and functions of two closely related interferon-inducible human genes, ISG54 and ISG56. J Biol Chem 2006;281:34064–71.

16. Ulker N, Samuel CE. Mechanism of interferon action. II. Induction and decay kinetics of the antiviral state and protein P54 in human amnion U cells treated with γ interferon. J Biol Chem 1987;262:16804–7.

17. Ulker N, Zhang X, Samuel CE. Mechanism of interferon action. I. Characterization of a 54-kDa protein induced by γ interferon with properties similar to a cytoskeletal component. J Biol Chem 1987;262:16798–803.

18. Saha S, Sugumar P, Bhandari P, Rangarajan PN. Identification of Japanese encephalitis virus-inducible genes in mouse brain and characterization of GARG39/IFIT2 as a microtubule-associated protein. J Gen Virol 2006;87:3285–9.

19. Boukamp P, Petrussevska RT, Breitkreutz D, et al. Normal keratinization in a spontaneously immortalized aneuploid human keratinocyte cell line. J Cell Biol 1988;106:761–71.

20. Blatch GL, Lassle M. The tetratricopeptide repeat: a structural motif mediating protein-protein interactions. Bioessays 1999;21:932–9.

21. Hendrix MJ, Seftor EA, Chu YW, Trevor KT, Seftor RE. Role of intermediate filaments in migration, invasion and metastasis. Cancer Metastasis Rev 1996;15:507–25.

22. Xu W, Zhang MW, Huang J, et al. Correlation between CK18 gene and gastric carcinoma micrometastasis. World J Gastroenterol 2005;11:6530–4.

23. Ajisaka H, Miwa K. Micrometastases in sentinel nodes of gastric cancer. Br J Cancer 2003;89:676–80.

24. Oshima RG, Baribault H, Caulin C. Oncogenic regulation and function of keratins 8 and 18. Cancer Metastasis Rev 1996;15:445–71.

25. Murant SJ, Handley J, Stower M, et al. Co-ordinated changes in expression of cell adhesion molecules in prostate cancer. Eur J Cancer 1997;33:263–71.

26. Seki N, Hattori A, Hayashi A, et al. Cloning, tissue expression, and chromosomal assignment of human MRJ gene for a member of the DNAJ protein family. J Hum Genet 1999;44:185–9.

27. Izawa I, Nishizawa M, Ohtakara K, et al. Identification of Mrj, a DnaJ/Hsp40 family protein, as a keratin 8/18 filament regulatory protein. J Biol Chem 2000;275:34521–7.

28. Carrigan PE, Sikkink LA, Smith DF, Ramirez-Alvarado M. Domain:domain interactions within Hop, the Hsp70/Hsp90 organizing protein, are required for protein stability and structure. Protein Sci 2006;15:522–32.

29. Stafford LJ, Vaidya KS, Welch DR. Metastasis suppressors genes in cancer. Int J Biochem Cell Biol 2008;40:874–91.

30. Friedl P, Wolf K. Tumour-cell invasion and migration: diversity and escape mechanisms. Nat Rev Cancer 2003;3:362–74.

31. Sakamoto S, Qin J, Navarro A, et al. Cells previously desensitized to type 1 interferons display different mechanisms of activation of stat-dependent gene expression from naive cells. J Biol Chem 2004;279:3245–53.

32. Wathelet MG, Clauss IM, Nols CB, Content J, Huez GA. New inducers revealed by the promoter sequence analysis of two interferon-activated human genes. Eur J Biochem 1987;169:313–21.

33. Yu M, Tong JH, Mao M, et al. Cloning of a gene (RIG-G) associated with retinoic acid-induced differentiation of acute promyelocytic leukemia cells and representing a new member of a family of interferon-stimulated genes. Proc Natl Acad Sci U S A 1997;94:7406–11.

34. Smith JB, Herschman HR. The glucocorticoid attenuated response genes GARG-16, GARG-39, and GARG-49/IRG2 encode inducible proteins containing multiple tetratricopeptide repeat domains. Arch Biochem Biophys 1996;330:290–300.

35. Miller CS, Johnstone BM. Human papillomavirus as a risk factor for oral squamous cell carcinoma: a meta-analysis, 1982-1997. Oral Surg Oral Med Oral Pathol Oral Radiol Endod 2001;91:622–35.

36. Chen PC, Kuo C, Pan CC, Chou MY. Risk of oral cancer associated with human papillomavirus infection, betel quid chewing, and cigarette smoking in Taiwan—an integrated molecular and epidemiological study of 58 cases. J Oral Pathol Med 2002;31:317–22.

37. Lung ML, Chan KH, Lam WP, et al. *In situ* detection of Epstein-Barr virus markers in nasopharyngeal carcinoma patients. Oncology 1989;46:310–7.

38. Creasey AA, Eppstein DA, Marsh YV, Khan Z, Merigan TC. Growth regulation of melanoma cells by interferon and (2′-5′)oligoadenylate synthetase. Mol Cell Biol 1983;3:780–6.

39. Interferon alfa-2a as compared with conventional chemotherapy for the treatment of chronic myeloid leukemia. The Italian Cooperative Study Group on Chronic Myeloid Leukemia. N Engl J Med 1994;330:820–5.

40. Lin SC, Liu CJ, Chiu CP, et al. Establishment of OC3 oral carcinoma cell line and identification of NF-κB activation responses to areca nut extract. J Oral Pathol Med 2004;33:79–86.

Molecular Cancer Research

IFN-Induced Protein with Tetratricopeptide Repeats 2 Inhibits Migration Activity and Increases Survival of Oral Squamous Cell Carcinoma

Kuo-Chu Lai, Kuo-Wei Chang, Chung-Ji Liu, et al.

Mol Cancer Res 2008;6:1431-1439.